eCommons (2019) https://doi.org/10.7298/vfyq-3506

6 Performance Evaluation

Lead Author: Shachak Pe'eri[a]

Contributing Authors: Christopher Parrish[b], Nicholas Johnson[c], Christopher Macon[c], and Stephen White[b]

a) Center for Coastal and Ocean Mapping, University of New Hampshire, Durham, NH 03824 USA;
b) Remote Sensing Division, National Geodetic Survey, NOAA, Silver Spring, MD 20901, USA
c) Joint Airborne Lidar Bathymetry Technical Center of Expertise, USACE, Kiln, MS 39556, USA

As with any survey system, it is strongly recommended that the service provider evaluate the performance of the ALB system prior to conducting the survey. The specifics of the evaluation can vary substantially based on user requirements and available resources. In this chapter, a general overview is provided regarding the approaches used for an ALB system performance evaluation. It is important to note that "performance evaluation" here refers to the tests that accompany the delivery of the ALB system from the manufacturer to the service provider, and that the approaches presented are based on the experience of U.S. government agencies and service providers. Some of the approaches reviewed below have been used with topographic lidar systems and for acoustic ship-borne transducers (namely, multibeam echosounders), but have not yet been tested with ALB systems. Although the manufacturer may have already conducted some calibration tests, it is important to repeat the procedures again using the service provider's aircraft. The six parameters that are used to evaluate the systems are: system health, noise evaluation, coverage evaluation, geometric calibration, accuracy evaluation and image/intensity quality evaluation (Beaudoin, Johnson, and Flinder 2013). In addition to acceptance, these parameters can be used as a baseline for future evaluation on the system, namely degradation or changes in the ALB system over time.

6.1 Expectations from the ALB systems

Every service provider, whether government agency or private sector company, is addressing a specific client or constituent group, and the performance expectations of a given ALB system are defined by the product specifications of the client. Although the primary product for most ALB surveys is bathymetry, the environmental conditions may vary and survey configurations may differ among service providers (LaRocque, Banic, and Cunningham 2004; Imahori et al. 2013). Technical and economic considerations limit the capacity of the ALB system to perform all the expected tasks at the same level of performance. Thus, prioritizing the specifications of the ALB system according to the specific mission is important.

As an example, two U.S. government agencies that use broad-beam ALB systems for coastal mapping have different requirements. The mission of the USACE National Coastal Mapping Program (NCMP) is to provide repetitive, regional, high-resolution, high-accuracy, seamless bathymetric-topographic data to support regional sediment management among coastal navigation, flood damage risk reduction, and ecosystem restoration projects. The program focuses on data collection where sediment is moving the most – along sandy coasts, and from the onshore dune system to the depth of closure (an offshore depth beyond which the depths do not change with time). USACE has broader data requirements on other types of coasts with a more extensive cross-shore expression than are addressed by other programs. These data, and a series of information products derived from them, are used to characterize engineering, environmental, and economic conditions along the shoreline, and their changes over time (Wozencraft 2014). USACE's mission also includes a requirement to monitor changes that occur naturally or due to manmade construction, which is typically over sandy areas. The USACE survey standards are that the ALB system should be able to acquire data at a spot spacing of $4m \times 4m$ with 100% coverage (i.e., no gaps in the survey flight plan) and achieve the same accuracy over the same area in the next survey cycle, which is every 5 to 7 years (Wozencraft 2010; USACE 2012). On the other hand, the goals of the NOAA ALB survey missions are to provide accurate, consistent, and up-to-date bathymetry and shoreline around the coasts of the U.S. and its territories (Imahori et al., 2013). The survey products need to meet international hydrographic survey standards, such as the IHO S-44 survey standards (IHO 2008). Accordingly, ALB survey data for hydrographic charting in NOAA are expected to: 1) fill in the data gap shoreward of the navigable area limit line (NALL) (0 to 4 m), and 2) overlap with surveys collected using sonar systems (e.g. multibeam, side scan or single beam) from 4 m to 10 m with a 0.5 m tolerance (Imahori et al. 2013). Many of coastal areas surveyed by NOAA include muddy, sandy and rocky coastal regions. The NOAA survey standards are that the ALB system should be able to acquire data up to a depth of 10 m at a spot spacing of $3\text{m} \times 3\text{m}$ with 200% coverage (i.e., two survey lines cover the same area). Also, each ALB survey needs to meet IHO order 1b standards (IHO 2008).

Theoretically, ALB systems can perform all the tasks mentioned above successfully. However, variations in environmental conditions (Chapter 3) and hardware degradation (Chapter 4) limit the ALB performance. A narrow-beam ALB will not provide successful bottom detection at depths greater than 10 m and broad-beam ALB systems do not provide spot spacing smaller than $2\text{m} \times 2\text{m}$. Thus, the service provider needs to identify and prioritize the tasks that the ALB system is expected to perform. In addition to the survey products, these tasks should include repeatability and degradation in performance over time.

6.2 Key Evaluation Parameters

6.2.1 System health

When delivering the ALB system, the manufacturer provides a list of specifications for the system. The list should include specifications for the laser, scanner, detection unit, and the auxiliary systems (e.g., positioning and attitude). Also, the manufacturer should provide recommended operational parameters on: operational altitude range, nominal aircraft speed, minimum eye-safe altitudes, temperature requirements and power requirements. Based on the system specifications and recommended operational parameters, it is possible to predict the swath width, the spot spacing and the ALB footprint diameter on the water surface.

It is also recommended that a full Built In Self Test (BIST) diagnostic routine be conducted at a calibration site (bench test), and then again after the system has been mounted in the aircraft on the runway prior to flying. The BIST provides the opportunity to perform measurements on the ALB system (i.e., laser, scanner, detector unit and auxiliary sensors) and to establish benchmarks for the health of the system components as they degrade with time. It is important to note that the BIST cannot provide a full characterization of the components as conducted at the manufacturer's laboratory facilities; however, this evaluation test provides a good indication of the overall ALB system's health. The BIST is particularly useful for monitoring the system health when conducted on a routine basis.

6.2.2 Noise evaluation

Mechanical and electrical noises may affect the ability of the ALB system to detect and track the seafloor using laser measurements. As with the tests described in the previous section (system health), a comprehensive noise analysis can only be conducted in an appropriate laboratory facility. However, a BIST diagnostic routine can be designed to assess if the aircraft platform is "quiet" (i.e., aircraft noise does not affect the recorded sensor measurements) and to determine if noise levels could be responsible for significant changes in the observations. The noise tests should be performed both statically on an optical bench, and again in flight (after the system has been mounted in the aircraft) at different speeds. Here, the signal-to-noise ratio (SNR) can be defined as the power ratio between the signal in the lidar return from a target, P_{signal} , to the background noise in the lidar return, P_{noise} , or as the square ratio of the amplitudes of signal, A_{signal} , and the background noise, A_{noise}:

$$SNR = \frac{P_{signal}}{P_{noise}} = \left(\frac{A_{signal}}{A_{noise}}\right)^2 \tag{6.2.1}$$

6.2.3 Swath coverage

The system health and noise tests evaluate only some of the factors that control the scanning performance of the ALB system. Swath coverage should be tested over different water depths in order to evaluate the achievable coverage and to compare it to a baseline performance level. As mentioned in Section 4.1.2, the swath width is dependent on the maximum off nadir angle across track and the height above the water surface. It is important to note that environmental conditions can also affect the achievable coverage (Section 3.3), and caution must be exercised when interpreting or comparing results from areas with different oceanographic regimes and/or seafloor composition (Beaudoin, Johnson, and Flinder 2013). A swath coverage test should include a land survey of a flat area (e.g., airport or football field) and a marine survey where the flight lines are running perpendicular to the depth contours. If the aircraft is able to maintain a constant height and fixed attitude angles, then the swath width should also be fixed throughout the survey line. Then, if any changes are observed in the swath width during the evaluation, further investigation of the cause is needed. Possible causes for the changes in the swath width over land are: synchronization issues between the ALB system and the auxiliary systems (Global Position System, GPS, and Inertial Navigation System, INS) (Wehr 2009), or calibration issues that include boresight-angle bias or offset, and biases of the laser beam range and angle calculations (Gonsalves 2010a; Habib 2009). It is important to note that the term Boresight Calibration mentioned later in this chapter refers to both spatial and orientations between sensors or between a sensor to the reference frame of the survey vessel, whereas boresight angles refer only to the orientation. Possible causes for the changes in the swath width underwater maybe related to an evaluation issue of the optical conditions underwater, variability of water conditions in a given swath (e.g. current causing differences in turbidity), or miscalculation of the optical geometry (Chapter 4).

eCommons (2019) https://doi.org/10.7298/vfyq-3506

6.2.4 Geometric calibration

Bathymetric data may contain geometric artifacts that can result from a number of sources. Two possible sources related to the system and/or ancillary sensors include: 1) faulty configuration of the systems in the aircraft, or 2) degradation in performance of the systems over time. Geometric calibration is the first of two procedures needed to confirm the quality of the acquired bathymetric data. The calibration procedure can be conducted over land (Gonsalves 2010a; Gonsalves 2010b). In that case, the system can be tested over a well-controlled environment without the need to correct for the sea surface morphology or distortions caused by the water column (Chapter 3). Geometric calibration serves to verify the relative contributions from the GPS, INS and the ALB system (Vaughn et al. 1996; Schenk 2001; El-Sheimy, Valeo, and Habib 2005; Habib et al. 2010). Misalignments would be expressed as translational or rotational offsets. This procedure is also common in acceptance tests for acoustic survey systems where it is known as a “Boresight Calibration” and will be discussed in more detail in Section 6.32.

6.2.5 Relative accuracy evaluation

After the geometric calibration has been accomplished, and the biases between the ALB system and the auxiliary systems are within survey specifications, a follow-up relative accuracy test is conducted. In essence, the relative accuracy test is a comparison of the ALB survey (conducted according the survey configuration defined by the service provider) to a reference acoustic survey (typically, a multibeam survey meeting IHO order 1a survey standards). In addition to an overall accuracy evaluation of the system as a function of depth, it is also possible to assess the accuracy of the laser measurements as a function of the scan angle (azimuth). The overall accuracy provides information on bottom detection and dependence on the environmental conditions. More details on the relative accuracy evaluation are provided in Section 6.33.

6.2.6 Radiometric evaluation

The amplitude of the return waveform, whether from the seabed or the water column, is another data product commonly available from ALB systems. The amplitude is commonly used to produce an image of bottom reflectance or column backscattering. Similar to bathymetry, any degradation of the health of the system, increase in noise or drift in calibration can degrade the quality of imagery. Image quality can be especially sensitive to transient noise events. Other potential sources of image artifacts include improper correction for range and water column attenuation. In contrast to bathymetric accuracy standards, there has not yet been a concerted effort to standardize the quality of ALB intensity imagery.

6.3 Evaluation tests

6.3.1 BIST

A typical BIST for multibeam systems is conducted on a ship at a dock with the engines off (Beaudoin, Johnson, and Flinder 2013). In contrast to multibeam systems, it is impossible to conduct such a test with an ALB system. Instead, it is recommended that, before the system is mounted to the plane, the ALB system should be tested by the manufacturer under laboratory conditions on an optical bench. The ALB system should be configured to measure a set of white and black targets at horizontal distances ranging from 300 to 500 m, a typical operational altitude range for ALB surveying. The manufacturer should supply the service provider with the waveforms (if available) and ranges in Laser file format (LAS). All of these observations should be compared to the distances and the reflectance values of the targets. The range measurements results should be within the tolerance values declared by the manufacturer. If possible, a transformation should be established between the reflectance measurements from the ALB (in arbitrary units) to the physical radiometric reflectance values of the targets measured by a spectrometer.

Next, the ALB system should survey at altitudes similar to the target ranges used in the bench measurement. A flat concrete or asphalt platform that is uniform in color (e.g., road or parking lot) can be used as a reference area. A set of survey lines in a cross-strip configuration should be collected at different speeds. From this evaluation survey, it is possible to conduct an analysis of the system performance for a set of ALB hardware parameters that include:

1. ***Swath width*** – The strip widths from different strips are compared in order to discern any changes in the swath width. It is also important to determine if the swath width is uniform along the strip.
2. ***Waveforms*** – The noise in the waveform should be evaluated with respect to the speed of the aircraft. Waveforms collected during the bench test measurement are used as a reference waveform that was collected in a "quiet" environment.
3. ***Ranges*** – The range distances of laser measurements of the same location on adjoining strips are evaluated. Systematic changes in range distance should be also compared to the incident angle.
4. ***Peak value (intensity)*** – The consistency of the bottom return shape characteristics and/or the intensity peak values of the laser measurements are evaluated. The average peak value and the variability in intensity within each strip are calculated and compared to the other strips. In addition to the peak value, the shape characteristics of the bottom return are evaluated as a function of the angle of incidence.

All the BIST results should be compared to the ALB system specification. It is recommended that the BIST results be shared with the manufacturer, highlighting any inconsistencies between the BIST results and either the ALB system specification or the BIST results from previous years. The manufacturer should discuss options for addressing any issues identified. All the BIST output results should be documented for comparison with the next BIST results.

6.3.2 Boresight Calibration (Geometric Calibration)

Organizations, such as IHO or ASPRS, have yet to standardize a Boresight Calibration procedure for ALB systems. Instead, the various geometric calibration procedures used for ALB systems are hybrids combining multibeam calibration procedures (OCS 2014; Beaudoin, Johnson, and Flinder 2013) and topographic lidar quality control procedures (Filin 2003; Habib et al. 2010; Toth 2009). Geometric calibrations for ALB systems are typically self-consistent, i.e. they do not require an external reference dataset. In contrast to standard calibration in photogrammetry, it is practically impossible to establish a direct correspondence between two point cloud datasets in overlapping multibeam or lidar calibration strips. Therefore, the data should be resampled for processing. Each laser measurement in the point cloud can be described by the general lidar geo-location equation (6.3.1) using the vector from the origin of the ground coordinate system to the INS body frame, $\vec{X}_0$, the offset between the laser unit and the INS body frame with respect to the laser unit coordinate system, $\vec{P}_G$, and the vector between the laser beam firing point and the target point, ρ. The ground position, $\vec{X}_G$, is derived by applying three rotation matrixes: the rotation matrix between the Inertial Navigation System (INS) body and the mapping frame, $R_{yaw,pitch,roll}$, the boresight matrix between the laser frame and the INS body frame, $R_{\Delta\omega,\Delta\phi,\Delta\kappa}$, and the scan angle rotation in the laser sensor frame, $R_{\alpha,\beta}$ (El-Sheimy, Valeo, and Habib 2005; Habib 2009):

$$\vec{X}_G = \vec{X}_0 + R_{yaw,pitch,roll} \cdot R_{\Delta\omega,\Delta\phi,\Delta\kappa} \cdot \vec{P}_G + R_{yaw,pitch,roll} \cdot R_{\Delta\omega,\Delta\phi,\Delta\kappa} \cdot R_{\alpha,\beta} \begin{bmatrix} 0 \\ 0 \\ -\rho \end{bmatrix} \tag{6.3.1}$$

A comparison between two calibration strips provides the 3D offset parameters that describe an affine transformation, The seven parameters that are required to define the geometric relationship between the point cloud in one strip to the point cloud in another strip include three parameters for the translation vector between the strips$(X_T, Y_T, Z_T)^T$, three for the rotation matrix for the co-alignment between the strips, $R_{\Omega,\Phi,K}$, and a scale factor, S:

$$\begin{bmatrix} x_{q_i'} \\ y_{q_i'} \\ z_{q_i'} \end{bmatrix} = \begin{bmatrix} X_T \\ Y_T \\ Z_T \end{bmatrix} + S \times R_{(\Omega,\Phi,K)} \begin{bmatrix} x_{q_i} \\ y_{q_i} \\ z_{q_i} \end{bmatrix} \tag{6.3.2}$$

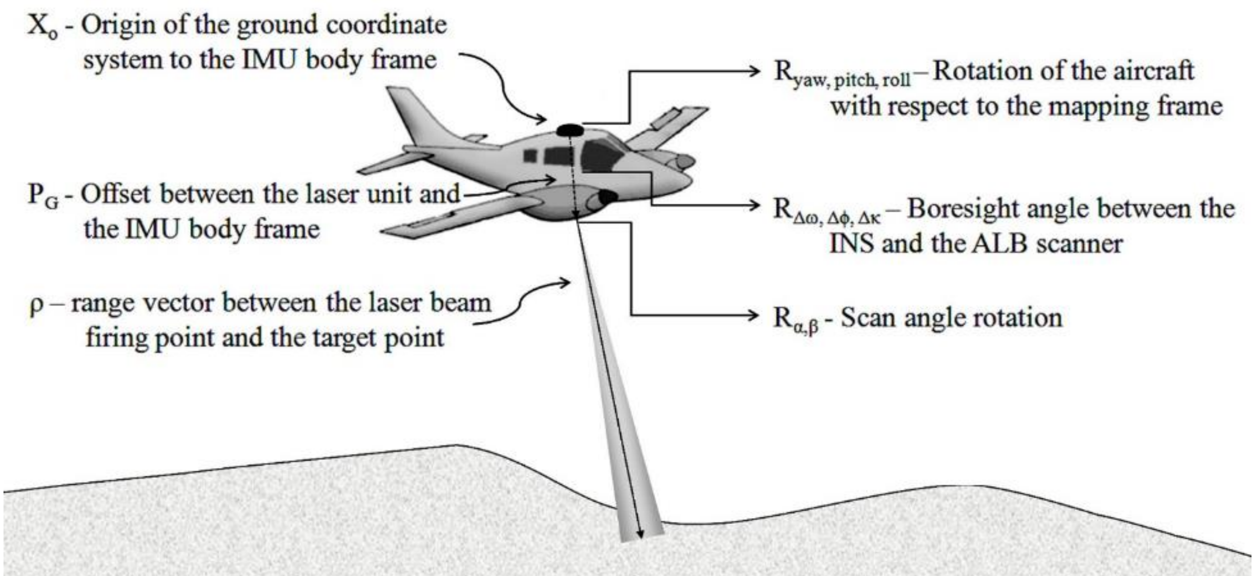

Figure 6.3.1. Geometric components for the general lidar geo-location equation.

It is recommended that the two calibration strips be collected over a flat terrain in order to provide the vertical offset, and over a prominent feature to provide the horizontal offset between the two datasets. The horizontal offset can also be evaluated by comparing the intensity images from the calibration strips. The calibration strips should be overlapping (ideally, 100% overlap). Also, it is assumed that the ALB strip does not contain synchronization issues in order to avoid any internal deformation within the strip. The internal deformation is defined for cases for which the rigid body model is not adequate to describe the relationship between the ground surface and the lidar system. Since geometric calibration will serve as a validation test for the measured offsets, it is required for both marine and aerial surveying in order to measure the lever-arm (position) offsets between a survey system to the GPS and INS systems. The lever-arm offsets measurement steps include the following recommendations (OCS 2014):

1) that the aircraft's approximate center of motion be coincident with the origin of the INS' local reference frame. This will reduce the number of physical offset measurements and, as a result, minimize the sources of error in position and attitude data.
2) that the horizontal and vertical distances to each of the sensors with respect to the origin of the INS' local reference frame will be determined by a professional surveyor using theodolites, laser range finders, total station, or optical levels. The service provider should consult with the manufacturer to define the specific accuracy requirements for the offset measurements between system components during installation.

For multibeam survey systems, the surveyed area that is used as a Boresight Calibration must either contain a prominent feature on the seafloor (e.g., rock or pipe) or be featureless, depending on the survey parameter that is investigated (Beaudoin, Johnson, and Flinder 2013). In a ship-borne survey, two survey lines in opposing directions are used to evaluate the attitude of the vessel, where roll and yaw are evaluated over any bottom profile, and pitch is evaluated over a sloping bottom. It is important to note that yaw evaluation requires the survey lines to completely overlap. Once the survey lines are acquired, carefully chosen subsets of the soundings are examined to systematically determine each calibration value. This procedure is commonly done manually, but there are, some software packages that offer semi-automated procedure (Gonsalves 2010a). The challenge in underwater geometric calibration is that line features, such as pipes, are difficult to find. As a result, many underwater Boresight Calibrations contain rocks as a prominent feature. Thus, the feature is observed with only one or two measurements, and those may not be representative of "the peak (least-depth) of the feature" (Gonsalves 2010b).

Quality assurance of topographic lidar is conducted from an airborne platform over land. Similar to the multibeam calibration procedure, topographic lidar calibration lines are acquired in pairs under the same survey conditions with a bias in one survey parameter between the lines (Vaughn et al. 1996; Schenk 2001; Filin 2003; El-Sheimy, Valeo, and Habib 2005; Habib 2009; Habib et al. 2010). The main difference between an underwater calibration procedure and a calibration over land is that potential errors related to the water surface and the water column (e.g., glint, refraction, and attenuation) are absent and prominent linear features (e.g., buildings with slope roofs) are more abundant (Gonsalves 2010b; Habib 2009).

Before conducting strip adjustment, well-defined reference areas, patches, are selected. In addition to the requirement that both strips should cover these reference areas completely, the patches should be evenly distributed across the swath of the strip in order to provide a strong geometric solution for the adjustment. The size of the patches depends on the point density, but is typically larger than 10 m for narrow-beam ALB systems with 2 to 5 pt/m^2, and 50 m for broad-beam ALB systems with 1/9 to 1/16 pt/m^2. Roads and parking lots are recommended features for patch areas. Also, moderately-sloped terrains or building structures can be used as patch areas. It is important to avoid vegetation that can cause multiple scattering within the biomass (such as shrubs or trees). Golf courses that contain lawn with very short grass can be used as patches if no other candidate patch areas are available. The water surface in a pond and a lake can

eCommons (2019) https://doi.org/10.7298/vfyq-3506

also be used as a patch; however, it is important that the water surface does not contain gravity waves (see Section 3.2).

There are a variety of strip adjustment approaches that can be grouped into five main categories (Habib 2009; Chen and Medioni 1992):

1. ***Gridded surface* -** The point clouds in both strips are converted into a surface. A comparison (matching of conjugate points) between the two grids allows one to calculate the deviation between the two strips. Gridding is typically used for surface generation for the whole strip, intensity point clouds, or for a patch area that contains multiple facets. Common grids use inverse distance weighted, natural neighbor interpolation, spline, or kriging interpolation methods.

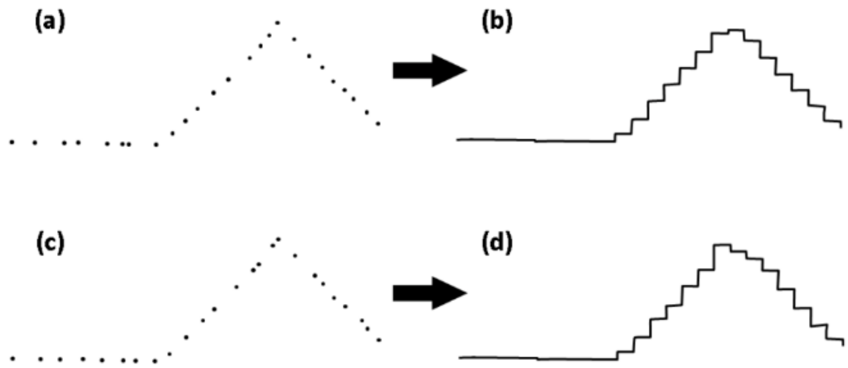

Figure 6.3.2. A schematic illustration of a gridded surface approach (side view in 2D). Point cloud from one strip (a) is compared to point cloud from an overlapping strip (c) by gridding the two point clouds (b and d, respectively) and comparing the surfaces.

2. ***Linear features* -** Linear features are extracted from the point clouds. These lines can be derived manually or automatically using an image processing algorithm, such as the Hough transform. Deviations from the optimum values (zero shifts, zero rotations, and unit scale factors) can be used as indications of systematic biases in the lidar system. It is important to note that only the orientation of the linear features must match; there is no requirement for the length of the features to match as well (i.e., the end point do not need to match).

eCommons (2019) https://doi.org/10.7298/vfyq-3506

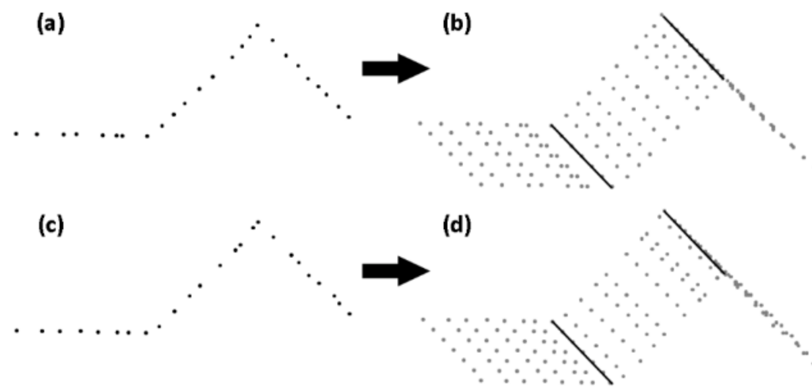

Figure 6.3.3. Schematic illustration of the linear features approach. A point cloud from one strip (a) is compared to a point cloud from an overlapping strip (c) by selection of linear features from overlapping surfaces between the two point clouds (b and d, respectively). Note: (a) and (c) are presented as a side views in 2D, whereas (b) and (d) are presented as an oblique views in 3D.

3. ***Iterative Closest Point (ICP)*** – Similar to linear features approach, it is possible to extract key points from point clouds of overlapping strips. By keeping a set key points from one strip fixed, an interactive calculation is used to estimate the rotation and translation of the second set using a mean squared error cost (i.e., minimum difference between two set of key points). After each rotation and translation estimation, the second set is transformed and then undergoes another iteration to re-associate the points until they two sets of key points converge to a threshold distance.

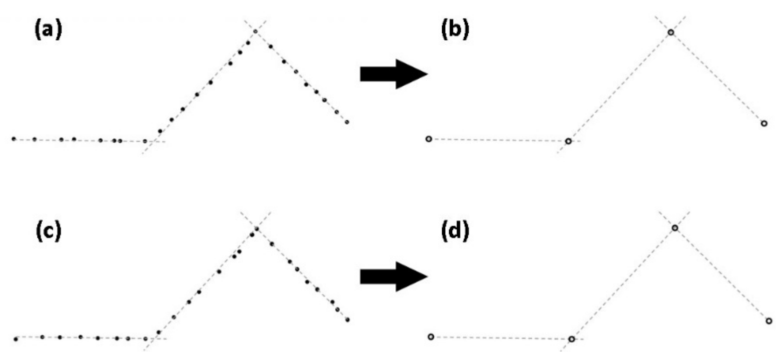

Figure 6.3.4. Schematic illustration of the ICP approach. A point cloud from one strip (a) is compared to a point cloud from an overlapping strip (c) by selection of key points from vertex point between the overlapping surfaces of the two point clouds (b and d, respectively).

4. ***Planar patches*** - Similar to the linear feature approach, planar patches can be used for matching. A least square adjustment is used to fit a planar surface from the point cloud. It is important that the reference area of the point cloud be identified as a flat surface. Also, the geometric calibration should include multiple patches at different slopes in order to have a strong solution to recover the transformation parameters.

eCommons (2019) https://doi.org/10.7298/vfyq-3506

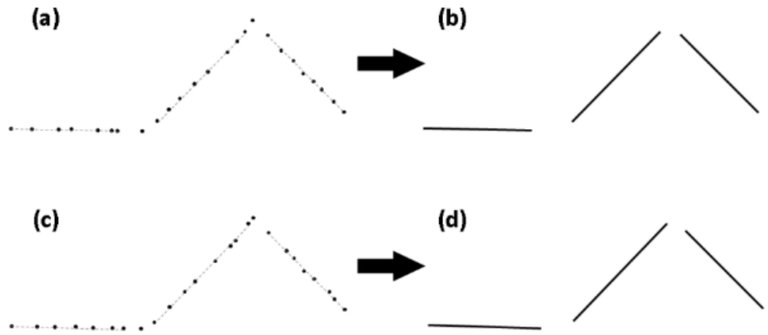

Figure 6.3.5. A schematic illustration of the planar patches approach (side view in 2D). A point cloud from one strip (a) is compared to a point cloud from an overlapping strip (c) by generating overlapping planar patches (flat surfaces) from the two point clouds (b and d, respectively).

5. ***Interpolated point cloud* -** An alternative approach to the gridded surface matching is resampling the point cloud in one ALB strip to match the location of the point cloud in the other strip. A surface is generated by a triangle irregular network (TIN).

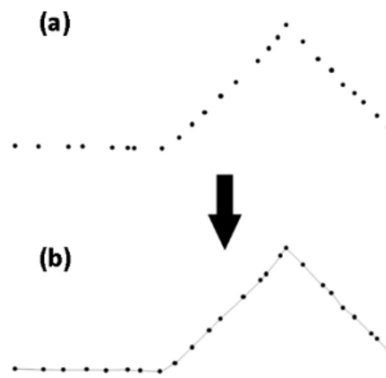

Figure 6.3.6. A schematic illustration of the Interpolated point cloud approach (side view in 2D). Point cloud from one strip (a) is used as a surface reference. Point cloud from an overlapping strip (b) is resampled horizontally based on the reference surface.

6.3.3 Relative accuracy Test

The relative accuracy test is an empirical comparison of the test data set against a reference data set that is assumed to be over a stable bottom (i.e., the reference data should be collected over a sandy bottom at the entrance to an inlet). The comparison results consist of a number of summary statistics that may include properties, such as mean, root mean square error (RMSE), and standard deviation, as well as histograms of differences. One of the goals of this test is to evaluate the performance of the ALB system in the field over a given seafloor type with a well-defined bathymetry. A multibeam echosounder or a dense single-beam echounder survey meeting the IHO order 1a survey standards is recommended as a reference bathymetry for evaluating a broad-beam ALB system in waters deeper than 3 m. For shallower depths

eCommons (2019) https://doi.org/10.7298/vfyq-3506

(< 2 m), bathymetry derived from a beach profiling survey is recommended for evaluating a narrow-beam ALB system. The relative accuracy test provides an evaluation for ALB surveying under typical water and weather conditions, such as a survey on a rising tide (flood stage) with winds less than 3.4 m/s (Beaufort sea stage 2 or less). The comparison between the two datasets is conducted after the ALB dataset has been edited and outliers have been removed. The evaluation consists of several steps that are conducted using tools available in commercial-off-the-shelf (COTS) software, such as ArcGIS, ENVI, CARIS, Fledermaus and MapInfo):

Preprocessing - In order to compare the ALB survey to the reference bathymetry, the ALB survey should be in a format that can be loaded into COTS software and have the same coordinate system as the reference bathymetry. The ALB data are typically acquired in a proprietary binary format. Two common, publicly available format types are ASCII format (e.g., XYZ or grid) and LAS format (ASPRS 2008a; ASPRS 2008b). The manufacturer typically provides a converter to parse the proprietary binary ALB data into one of these two, allowing them to be loaded into COTS software.

The comparison between the ALB and reference data should be in the same vertical and horizontal system. It is important to note that ALB surveys are referenced to an ellipsoidal or orthometric vertical datum, whereas the reference bathymetry might be referenced to a tidal datum. If sufficient tidal data is not available for chart datum transformation, the comparison should be done in the ellipsoidal or orthometric vertical system. A similar situation may also occur with the horizontal system, where one dataset uses geographic units (i.e., longitude and latitude) and the other dataset is projected using northing and easting coordinates. Figure 6.3.8 provides an example of a transformation flow diagram from the JALBTCX ALB survey data coordinate system (geographic horizontal system and an ellipsoidal North American Datum 1983 (NAD83) vertical system) to the reference system of the NOAA multibeam echosounder survey (Universal Transverse Mercator (UTM) projected horizontal system and a tidal Mean Lower Low Waters (MLLW) vertical system) using NOAA's VDatum transformation tool (White 2007).

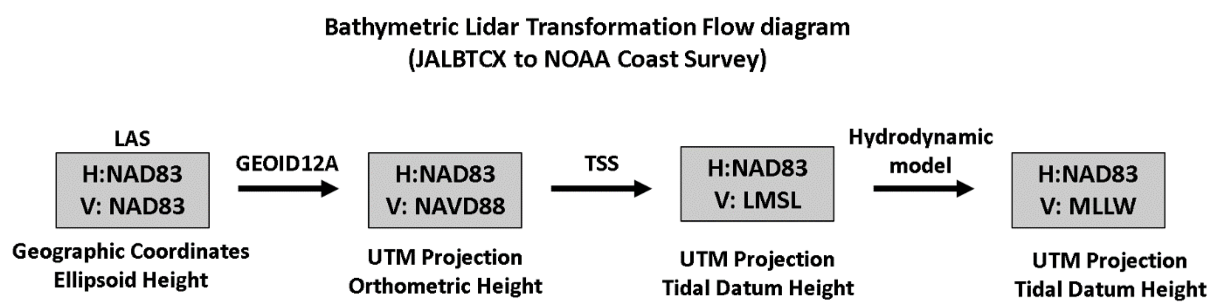

Figure 6.3.7. Transformation flow diagram of NCMP lidar data from JALBTCX archives (USACE – JALBTCX), to NOAA's Office of Coast Survey (OCS). NAD83 – North American Datum 1983; NAVD88 – North American Vertical Datum 1988; LMSL – Local Mean Sea Level; MLLW - Mean Lower Low Waters; TSS – Topography of the Sea Surface; UTM - Universal Transverse Mercator.

Density map - Coverage maps with density values (number of laser measurements per square meter) provide spatial information on the ALB performance that includes areas with low or no bottom detection. These density maps allow the operator to intersect these maps with the

eCommons (2019) https://doi.org/10.7298/vfyq-3506

reference bathymetry and infer the effective operation depth of the ALB system and its performance over different strata (Figure 6.3.8). The average spot spacing, which is a function of the density can be also calculated as a function of depth. For example, an ALB survey with a $4\ \mathrm{m} \times 4\ \mathrm{m}$ spot spacing is equal to a density of $(1/16) = 0.06\ \mathrm{pts/m^2}$. Figure 6.3.8 presents two examples of density maps (Imahori, Ferguson, Wozumi, Scharff, Pe'eri, Parrish, White, Jeong, Sellars, Aslaksen, et al. 2013). On the left is a density map of a USACE SHOALS survey over an area near Port Everglades, FL (2009). The density map shows a uniform distribution that ranges between 0.06 to 0.17 pts/m^2, which is typical for a survey using this type of ALB over a sandy coral bottom with clear water conditions. On the right is a density map of a 2007 USACE SHOALS survey over an area near Kittery, ME. The density map is patchy with a density that ranges 0.04 to 0.13 pts/m^2. Such density map characteristics may be attributed to the seafloor type (sandy with rocky outcrops) and the water clarity (~0.2 m) (Pe'eri et al. 2011).

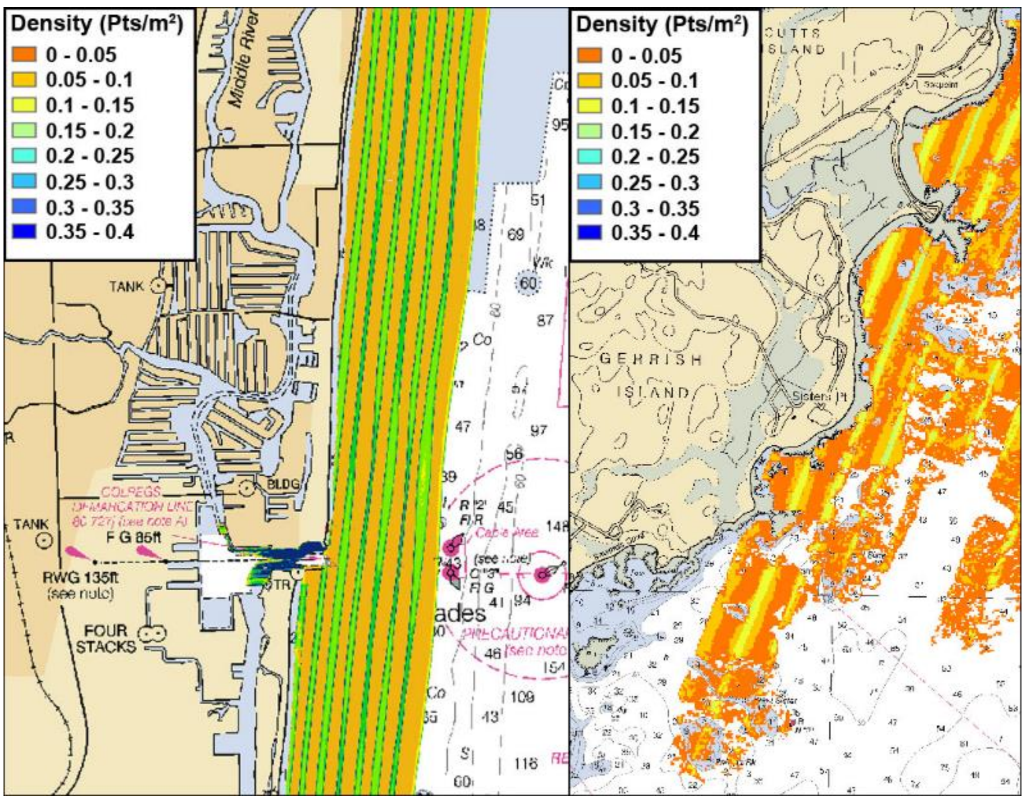

Figure 6.3.8. Density maps of USACE CHARTS system (Imahori, Ferguson, Wozumi, Scharff, Pe'eri, Parrish, White, Jeong, Sellars, Aslaksen, et al. 2013): (left) Port Everglades, FL (2009) and (right) Kittery, ME (2007).

Difference map - It is important to note that, before generating a difference map, both datasets should be in the same horizontal and vertical systems. Also, both datasets should be gridded to a scale smaller than the spot spacing. Otherwise, the interpolation method will affect the results and aliasing may occur. A difference map of derived elevations can be generated by the subtraction of the ALB bathymetry grid from the reference bathymetry grid. In addition to the accuracy of the systems, spatial changes in the difference between the two datasets may indicate an actual change in bathymetry (e.g., over tidal inlets) or spatial variability of water clarity or the seafloor type (Figure 5.3.6.3.10). It is also important to note that some hydrographic offices consider a systematic bias of up to 0.2 m to be a reasonable difference between ALB surveys and the reference bathymetry. Figure 5.3.9 presents two examples of difference maps (Imahori, Ferguson, Wozumi, Scharff, Pe'eri, Parrish, White, Jeong, Sellars, Aslaksen, et al. 2013). On the left is a density map showing the difference between a 2009 USACE SHOALS survey and a 2008 NOAA MBES (Multibeam Echo Sounder) survey (Ocean Surveys 2009) over an area near Port Everglades, FL that contains a stable seafloor (bathymetry changes are mainly due to major weather events). The depth difference between the two datasets is uniform (standard deviation of 0.24 m) with a small average (0.54 m). On the right is a difference map between a 2004 USACE SHOALS survey and a 2008 NOAA MBES over a tidal inlet near Pensacola, FL. The depth difference map in this case is not uniform (standard deviation of 1.72 m with an average difference of 0.57 m) and indicates that the bottom morphology has changed during the 5 years between the two surveys.

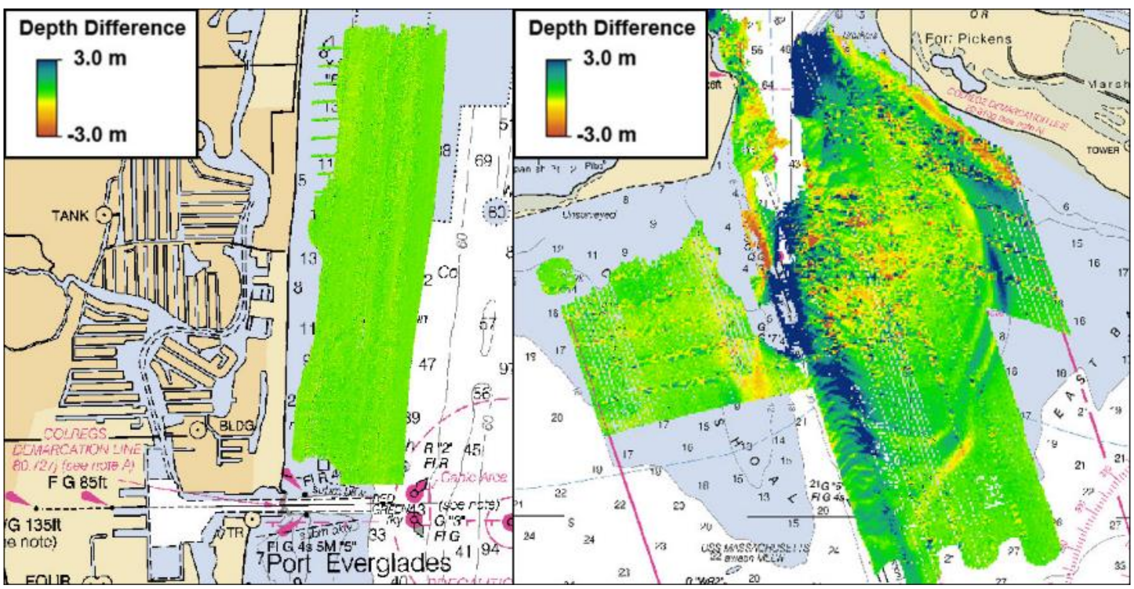

Figure 6.3.9. Difference maps between USACE CHARTS surveys to NOAA multibeam surveys: (left) Port Everglades, FL and (right) a tidal inlet near Pensacola, FL.

Histogram - For a general evaluation of the whole survey area, or for only a subset section, the histogram provides a visual aid showing the difference frequency between the two datasets (Figure 6.3.10). The mean and standard deviation indicate if there is a systematic offset (especially, if the two dataset have not been referenced correctly) and the value of the measurement error. Figure 5.3.10 illustrates the difference distribution for the two USACE SHOALS surveys presented in Figure 5.3.9.

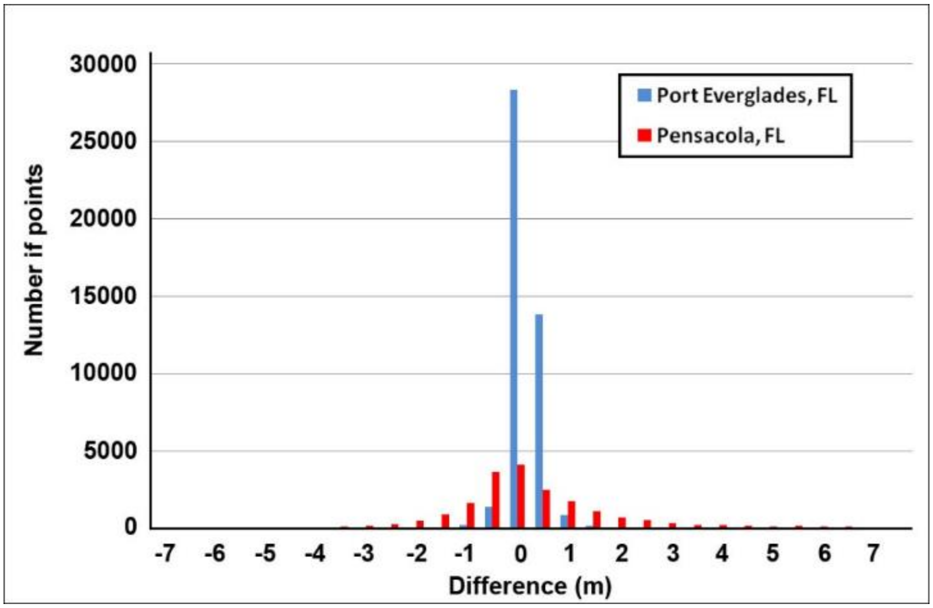

Figure 6.3.10. Histograms for the data presented in Figure 5.3.9 of the depth differences between the USACE CHARTS surveys of Port Everglades, FL acquired in 2009 (blue bars) and Pensacola, FL acquired in 2004 (red bars) compared to NOAA multibeam survey data from 2008, respectively.

Scatter plot - When the difference values between the two datasets are intersected with the depth values, it is possible to evaluate the ALB performance as a function of depth (Figure 6.3.11). The scatter plot also provides a mean and standard deviation that can be segmented as a function of depth. It is common to notice an increase in standard deviation over very shallow coastal areas (less than 1 meter) because of wave action and suspended particulates. Figure 6.3.11 shows a scatter plot comparison between a CHARTS ALB survey from 2012 conducted by the USACE, and a LADS MKII ALB survey from 2009 conducted by NOAA. The scatter plot shows an overall good agreement in depth. The overall mean and standard deviation (1σ) are 0.17 m and 0.32 m, respectively. An investigation of depth difference measurements as a function of depth in the scatter plot shows the standard deviation is less than 0.5 m at depths ranging from 3 m up to 20 m. At depths shallower than 3 m, the standard deviation increases to more than 1.0 m. This may be attributed to coastal processes (e.g., breaking waves). Accordingly, it is better to conduct the relative accuracy over bottom depths deeper than 2 m.

eCommons (2019) https://doi.org/10.7298/vfyq-3506

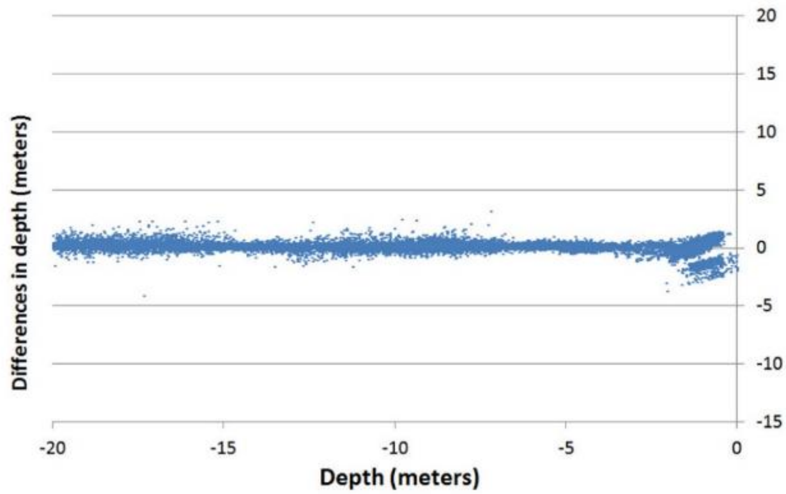

Figure 6.3.11. Histogram of the depth difference between a CHARTS ALB survey from 2012 conducted by the USACE and LADS MKII ALB survey from 2009 contracted by NOAA.

Results from the accuracy test are checked against hydrographic survey standards (e.g., IHO or USACE) and system performance defined in the service provider's requirements:

Depth penetration - The depth penetration capability (maximum depth) is a performance requirement based on the diffuse attenuation coefficient, K_d, combined with a depth requirement, d and is dependent on the survey capabilities of the service provider. Some require an absolute depth requirement (e.g., 10 m) because the ALB survey will overlap with an acoustic survey with a criterion of $K_d * d > 1$. Others may plan to use the ALB system measurements alone, which would require a $K_d * d > 3$ criterion.

Vertical accuracy - The total vertical accuracy (TVU) underwater is typically evaluated based on the IHO S-44 standards (IHO 2008). The IHO TVU describes the 95% confidence level of the measurements and is dependent on the IHO order coefficients (Table 5.1), *a* and *b*, and the water depth, *d*:

$$\sqrt{a^2 + (b * d)^2} \qquad (6.3.3))$$

Table 6.1. TVU Coefficient values for the different IHO orders (IHO 2008)

IHO order	a	b
Special	0.25	0.0075
1	0.5	0.013
2	1.0	0.023

Horizontal accuracy - The total horizontal accuracy (THU) underwater for an ALB survey describes the 95% confidence level of the measurements and is also typically evaluated based on the IHO S-44 standards (Table 6.2):

eCommons (2019) https://doi.org/10.7298/vfyq-3506

Table 6.2. THU values for the different IHO orders (IHO 2008)

IHO order	THU
Special	2 m
1	5 m + 5%*d
2	20 m + 10%*d

6.3.4 Output formats

Typically, the manufacturer provides processing software that can post-process the lidar raw observations (waveforms) with the auxiliary systems. However, additional software is required for surface analysis or for further processing of the referenced point cloud data with additional data (e.g., seafloor character maps, information of marine protected areas, location of navigational channels and anchorage areas). Common software include: ArcMap, Global Mapper, Caris, Fledermaus, PFMabe and AutoCad Map. In order to load the data into these software packages, the laser measurements need to be converted from a proprietary format (i.e., a file structure intended for internal processing and is not open to the public) into a conventional exchangeable binary format or a common ASCII format.

The simplest form for an output file is ASCII format, such as XYZ or ESRI GRID format. The challenge of using ASCII format is that these are very large files that can fill the data archive or storage device with less survey coverage than would be achieved with a survey file in a binary format. Instead, LAS format files are commonly used as a deliverable format. These files are binary and contain a specific structure that is defined by the American Society for Photogrammetry and Remote Sensing (ASPRS 2010). Documentation for the LAS format is publically available allowing vendors and customers to export and import the data between different software. To date, ASPRS has published a fourth revision of the LAS format specification (LAS 1.4) since its initial version 1.0 release (ASPRS 2008b). In addition to XYZ, the LAS 1.4 format provides a header block, variable length records (VLR), extended variable length records (EVLR), and a full point data record (Table 6.3). The header block provides information on the survey, calibration parameters of the ALB system, and how to read the information in VLR and EVLR. Any additional information that the manufacturer or the service provider are interested in providing (e.g., full waveforms) can be recorded in the VLR and the EVLR. The VLR block is used by vendors that wish to maintain legacy compatibility. If the vendors are not concerned with legacy LAS reader software, then the EVLR can be used to store auxiliary information, especially to update information (normally contained within a VLR) without the need of rewriting the point data block. The most used block in LAS is the full point data record that, in addition to XYZ information, contains information on the intensity, return number, number of returns (given pulse), scan direction flag, edge of flight line, classification, scan angle rank, and user defined data for each point.

eCommons (2019) https://doi.org/10.7298/vfyq-3506

Table 6.3. LAS 1.4 Format Definition (ASPRS 2008b)

PUBLIC HEADER BLOCK
VARIABLE LENGTH RECORDS (VLR)
POINT DATA RECORDS
EXTENDED VARIABLE LENGTH RECORDS (EVLR)

It is recommended that the service provider verify the LAS versions that are currently available in the lidar processing software used for import and export operations. There is the possibility that import and export LAS files are in different LAS versions. It is also recommended that the lidar files be exported into LAS during the acceptance test procedures and to verify that all key parameters are exported. This verification can be done with one of the COTS software packages (e.g., LAStools or LP360).

6.4 Examples of Performance Evaluations

It is hard to find documentation of ALB field acceptance tests in the open literature. This is because BIST and geometric calibration tests are typically reported as result tables or as internal company reports and only a few of the relative accuracy tests are published as conferences proceedings. This section provides examples on several of the ALB systems based on published reports and personal communication with manufacturers. It is important to note that while the previous section provided theoretical background for an ideal situation (no budget or time constraints), the goal of this section is to provide a realistic perspective using examples of acceptance tests conducted by service providers and manufacturers.

6.4.1 USACE/Navy performance evaluation tests

Over the past 20 years, the USACE and the Navy have conducted performance evaluation tests on different ALB systems in the process of either acquiring the system or using service providers that operate such ALB systems. Two of the most recent ALB systems purchased by the USACE were the SHOALS-1000T/3000 and the CZMIL systems. A SHOALS-1000T/3000 evaluation test was conducted by the USACE and the U.S. Navy (Optech 2005). The goals of the test were to evaluate depth penetration capability (maximum depth), vertical accuracy underwater and horizontal accuracy underwater. Specifically, the USACE and U.S. Navy evaluated the ability of SHOALS-1000T to meet IHO Order 1 standards (IHO 2008), to detect the bottom based on a $K_d * d > 3$ (K_d is the diffuse attenuation coefficient and d is depth) criteria, and to perform topographic coastal mapping.

The BIST procedure for the SHOALS included two tests conducted at the Optech facilities in York, ON, Canada. The first BIST test was a dry run (i.e., the laser unit was not active) using an optical simulator. Laser pulses were generated using a board containing diodes that acted as a signal generator (Figure 6.4.1). The input parameters for Optech's Optical Simulator were: survey altitude of the aircraft, water depth, amplitudes of the bottom and surface returns, and false return range (Optech 2005). The laser pulses were used to test both the scanner unit and the detector unit. After validating all the electro-optical components in the dry run, the ALB system was tested using the transmitter unit over a target at a known distance (~80.0 m) and through a fiber optic cable. The next step, a test from an optical bench (not from an air craft) at operational ranges (300 to 500 m), was complicated by the need to maintain eye safety.

eCommons (2019) https://doi.org/10.7298/vfyq-3506

The solution was to conduct the second BIST by transmitting the laser pulses through a spool of fiber optic cable. Optech calls this configuration a "laser power timing test", where structure and timing of the pulse were tested in a well-controlled environment. An additional benefit of the laser power timing test is the ability to radiometrically characterize the system's detectors and calibrate new replacement detectors to the specifications of the previous ones. After the BIST, the SHOALS system was mounted in a Beechcraft King Air 90 and was flown over Oshawa or Peterborough airports, which are located near Toronto, CA. The airport runway and local structures (namely, buildings) were used for calculation of the boresight angles.

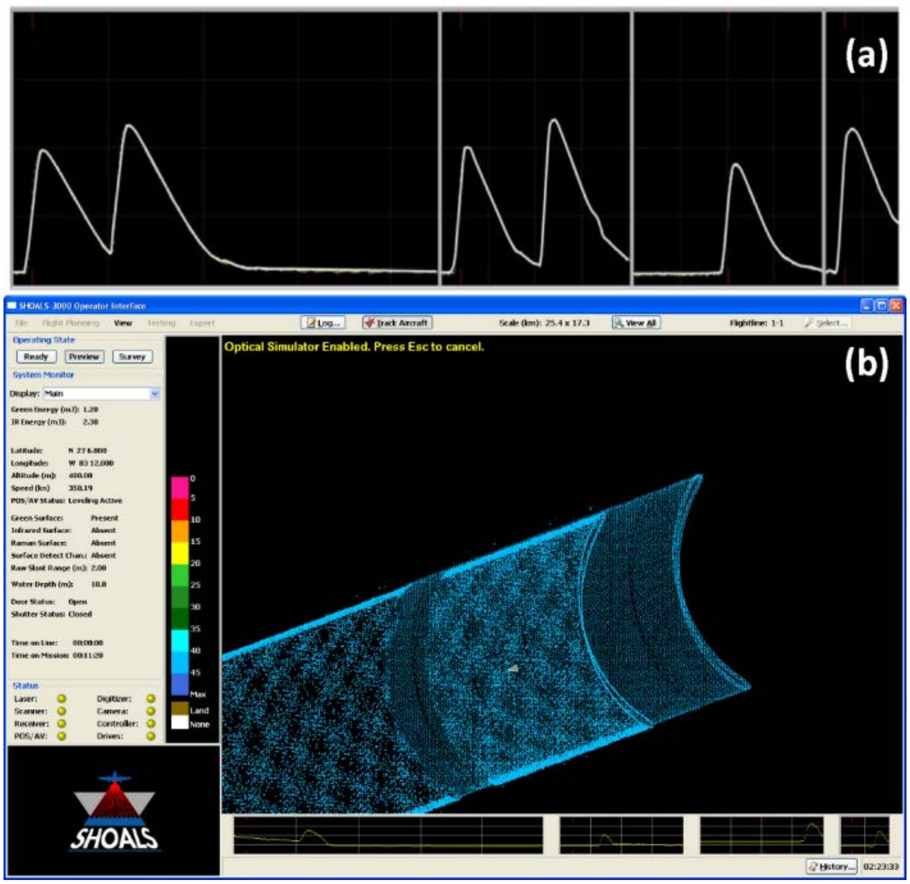

Figure 6.4.1. Optech's Optical Simulator: (a) Typical waveforms, and (b) screen shot of a BIST using the optical simulator.

USACE's and U.S. Navy's relative accuracy tests of the SHOALS-1000T (also known as Compact Hydrographic Airborne Rapid Total Survey, CHARTS) were conducted over the Naval South Florida Testing Facility (SFTF), Fort Lauderdale, FL, USA. The system was tested in several aircraft including: Beechcraft King Air 90, Beechcraft King Air 200, Beechcraft King Air 350, and deHavilland Twin Otter. The acceptance tests were conducted during July 2003, and were compared to a reference bathymetry that was collected using Kongsberg EM-1002 and EM-3000 multibeam system. In addition, ground truth data were collected using sidescan sonar and *in situ* spectral measurements of the water column. The ALB survey data was tide coordinated and was converted from WGS-84 to MLLW using a NOAA tide gauge that was located 20 miles south of the study site (Virginia Key, FL).

The results were an evaluation of the depth penetration capability of SHOALS 1000T in three locations. In addition, the depth penetration of the lidar system was predicted using an ocean optical model (Ocean Scientific 2003). A maximum depth was calculated to be around 45 m based on the density of the laser measurement criteria from lidar survey. The depth penetration results (Table 5.4) showed that the ALB system met the $K_d * D > 3$ requirement. The horizontal and vertical accuracies were evaluated using ten sites, all with depths less than the maximum penetration depth. The empirical error at each site was calculated as the sum of the mean (μ) with two standard deviations (2σ) of the depth differences between the ALB and the MBES surveys (i.e., $\mu + 2\sigma$). The resulting errors were compared to the IHO order 1 95% specification. Both the vertical and horizontal accuracy results showed that the ALB system meets the IHO order 1 requirement in most cases.

Table 6.4. Depth penetration results (shoals-1000T) (Optech 2005)

Laser measurement depth (m)	$\boldsymbol{K_d}(\boldsymbol{m^{-1}})$	$\boldsymbol{K_d}$d
-39.40	0.08	3.15
-44.45	0.10	4.45
-39.79	0.10	3.98

Based on the experienced gained using the SHOALS system, the USACE adopted part of the Interagency Working Group's National Coastal Mapping Strategy as a new set of survey standards, known as quality levels (QL) (Table 5.5; Figure 5.3.13). The vertical accuracy and planned spot spacing density determine the QL. The goal of the new survey standards is to match the U.S, Geological Survey (USGS) 3D Elevation Program (3DEP) topographic survey standards on land (Dewberry 2012; Snyder 2012) and the IHO S-44 standards at water depths greater than 20 m (IHO 2008). It is also important to note that the vertical USACE quality level scale is for vertical uncertainty evaluation and not object detection in order to match IHO specifications (IHO order 1b). The USGS Quality Levels were defined using RMSE terms to match the IHO definitions (95% confidence level). The IHO TVU definitions were converted to RMSE based on the assumption that the distributions are Gaussian.

Table 6.5. Vertical USACE Quality level definitions for ALB Surveys, where *D* is the water depth in meters.

Bathy Lidar Quality Level	Point Density (pt/m^2)	Nominal Pulse Spacing (m)	Vertical RMSE (m)
QL1B	1.00	1.0	0.095 + 0.00275D
QL2B	0.25	2.0	0.095 + 0.00275D
QL3B	0.25	2.0	0.185 + 0.00275D
QL4B	0.04	5.0	0.185 + 0.00275D
QL5B	0.04	5.0	0.463 + 0.00275D

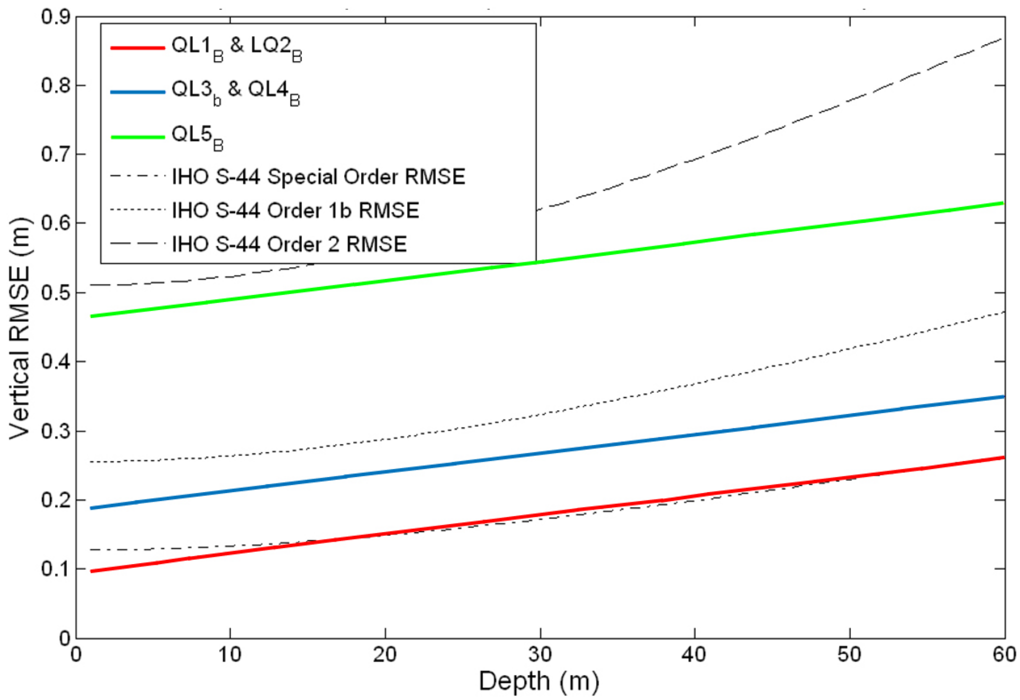

Figure 6.4.2. Vertical RMSE plots describing USACE lidar vertical quality level definitions with respect to the IHO survey standards.

The performance evaluation tests for the CZMIL system were conducted by the USACE and the Navy. The systems were mounted on a Beechcraft King Air 200. Geometric calibration of the CZMIL was conducted during June, 2013. A coarse boresight angle evaluation was conducted over the water surface (offshore Bay St. Louis, MS). After a rough approximation of the boresight angles from the offshore survey, a second ALB survey was conducted over Stennis airport, Kiln, MS (Figure 5.3.14). The flat airport runway makes it possible to calculate errors/uncertainties manually and/or automatically using numeric analysis. All the geometric parameters were then evaluated over structures with pitched roofs. The ALB datasets were compared to ground truth reference datasets. The airport runway was measured using an Optech Lynx Mobile Mapper (range precision of 5 mm at 1σ) survey from October of 2011 with a laser point density of 571 pts/m^2. Several pitched roofs were measured using a Trimble VX Spatial Station. Both ground truth surveys were referenced using Trimble R8 RTK data on an NGS published control monument (BH2999). In addition to a geometric calibration, an average point density on land of 2.17 pts/m^2 was calculated for a section in the middle of the swath over a flat area. This high point density value for the CZMIL is attributed to the 7 laser measurements for each transmitted pulse and the circular scanning that provides forward and backward-looking scans over the same area. The comparison results between the ground truth data and the CZMIL survey were in good agreement (Figure 5.3.14 right image).

eCommons (2019) https://doi.org/10.7298/vfyq-3506

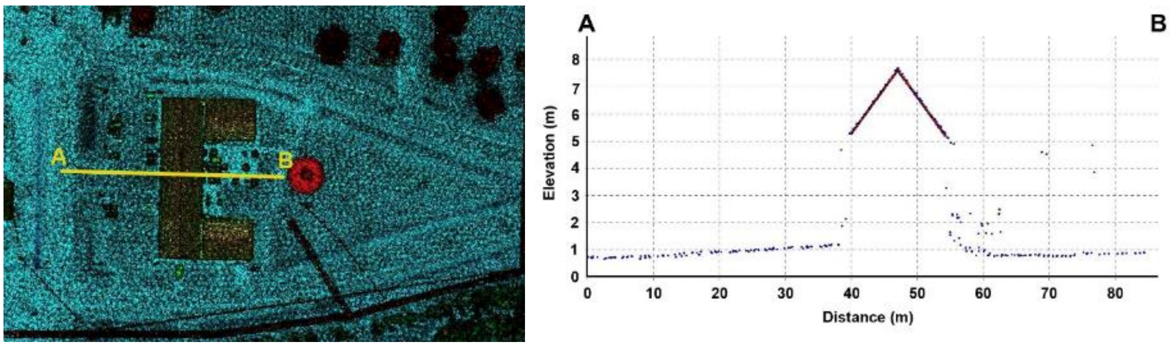

Figure 6.4.3**.** Geometric calibration of the CZMIL data: (Left) elevation map of Stennis, MS and (right) side profile over the JALBTCX facility. The black lines were calculated based on measurements conducted by Trimble VX Spatial Station.

The relative accuracy tests for CZMIL were conducted by the USACE in two locations: offshore Bay St. Louis, MS, USA (June, 2013) and over the SFTF, Fort Lauderdale, FL, USA (August, 2013). In both flights, the CZMIL system was mounted in a Beechcraft King Air 200. Although MBES surveys were conducted as reference for the acceptance test, a hydrographic level bathymetry has not yet been produced (the survey was undergoing revision during the publication time of this section). Instead, bathymetry generated from the CHARTS acceptance test dataset over Fort Lauderdale, FL, USA was used as a reference (June-July, 2005). The CZMIL surveys were conducted at 200% coverage with a spot spacing of $2\ m \times 2\ m$. A maximum depth was calculated to be around 30 m based on the density of the laser measurement criterion from the lidar survey. Due to potential changes in shallow water bathymetry during the 8 years between the surveys, the bathymetry datasets were compared at depths greater than 5 m. The preliminary results, using more than 4.5 million laser measurements, showed a 2σ standard deviation of 0.20 to 0.29 m with a 0.11 m RMSE for the Shallow channel measurements and a 2σ standard deviation of 0.33 to 0.34 m with a 0.17 m RMSE for the Deep channel measurements (Table 5.6; Figure 5.3.15). The point density of the central shallow channel (i.e., one laser measurement per laser pulse) at a 200% coverage was 0.26 pts/m^2. Further work is expected this year (2014) before recommendation for operation can be made.

Table 6.6. Preliminary results for CZMIL (Ft. Lauderdale, FL).

	Shallow channel		Deep	
	2σ	RMSE	2σ	RMSE
130507_1742	0.20 m	0.11 m	0.34 m	0.17 m
130509_2023	0.21 m	0.11 m	0.33 m	0.17 m
130509_2334	0.29 m	0.11 m	0.33 m	0.17 m

eCommons (2019) https://doi.org/10.7298/vfyq-3506

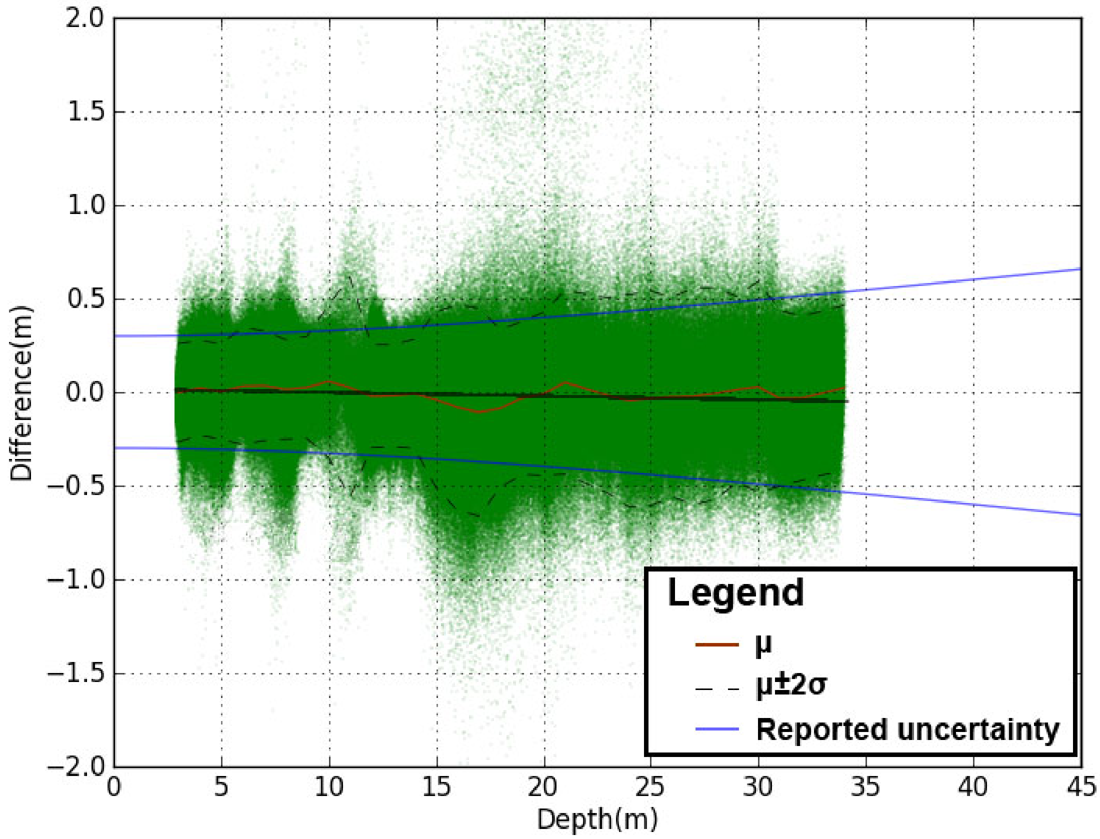

Figure 6.4.4**.** Scatter plot from a relative accuracy test for the deep channel measurements of CZMIL system.

6.4.2 NOAA performance evaluation tests

NOAA also evaluated the SHOALS-1000T system. A performance evaluation test was conducted by NOAA and Fugro Pelagos (Lockhart, Dushan, and Millar 2005; Fugro Pelagos 2008). Similar to the USACE, the goals of the NOAA test were also to evaluate depth penetration capability (maximum depth), vertical accuracy underwater, and horizontal accuracy underwater. However, the survey standards of the USACE and NOAA tests were different. The USACE and U.S. Navy tests compared the results to meet IHO Order 1 standards (IHO 2008) and a penetration depth of $K_d * d > 3$ (K_d is the diffuse attenuation coefficient and d is depth), whereas the NOAA and Fugro tests evaluated how well the ALB accuracy test met different levels of IHO standard (i.e., Special order, Order 1 or Order 2) and if an ALB survey at 200% coverage could be used with a Combined Uncertainty and Bathymetric Estimator (CUBE) algorithm. NOAA did not require an evaluation for topographic applications from the SHOALS-1000T system.

The NOAA and Fugro performance evaluation tests were conducted over the Shilshole Bay near Seattle, WA, USA using a Beechcraft King Air 90 aircraft (Figure 5.3.16). The tests were conducted during August, 2007 and were compared to a reference bathymetry collected in 2005 using a Reson 8101 multibeam system. These tests included survey lines over the same area collected at different altitudes

eCommons (2019) https://doi.org/10.7298/vfyq-3506

(300 m and 400 m) and spot spacings (3 m X 3 m, 4 m X 4 m, and 5 m X 5 m). The ALB survey data were tide coordinated and converted from WGS-84 to mean low lower water (MLLW) using a NOAA tide gauge that was located near the study site (Port of Seattle, WA).

A geometric calibration was conducted prior to the relative accuracy tests. Two ground GPS base stations were used in the geometric calibration. The two stations provided both quality control and redundancy in the event that one of the two systems was disturbed or the equipment experienced a failure. The aircraft remained within 30 km of an operational base station at all times during survey. The internal positioning solution was determined using Applanix POSPac. After the geometric calibration, survey data collected for the accuracy tests were compared to bathymetry derived from the MBES survey. The accuracy results showed that the mean difference ranged between -0.14 m to 0.07 m with a standard deviation of about 0.12 m to 0.13 m. Results from a statistical analysis of the survey datasets indicated that the survey data from SHOALS-1000T can meet IHO order 1 standards (S-44 version 4; (IHO 2008). However, SHOALS-1000T survey data at 200% overlap provides only a single weak solution (primary solution) in CUBE for the detection of small shallow features. This is likely because of data sparseness and the size of the ALB footprints. As a result, the seafloor surface may not be accurately represented for all shallow areas captured within the point cloud dataset and further work is required.

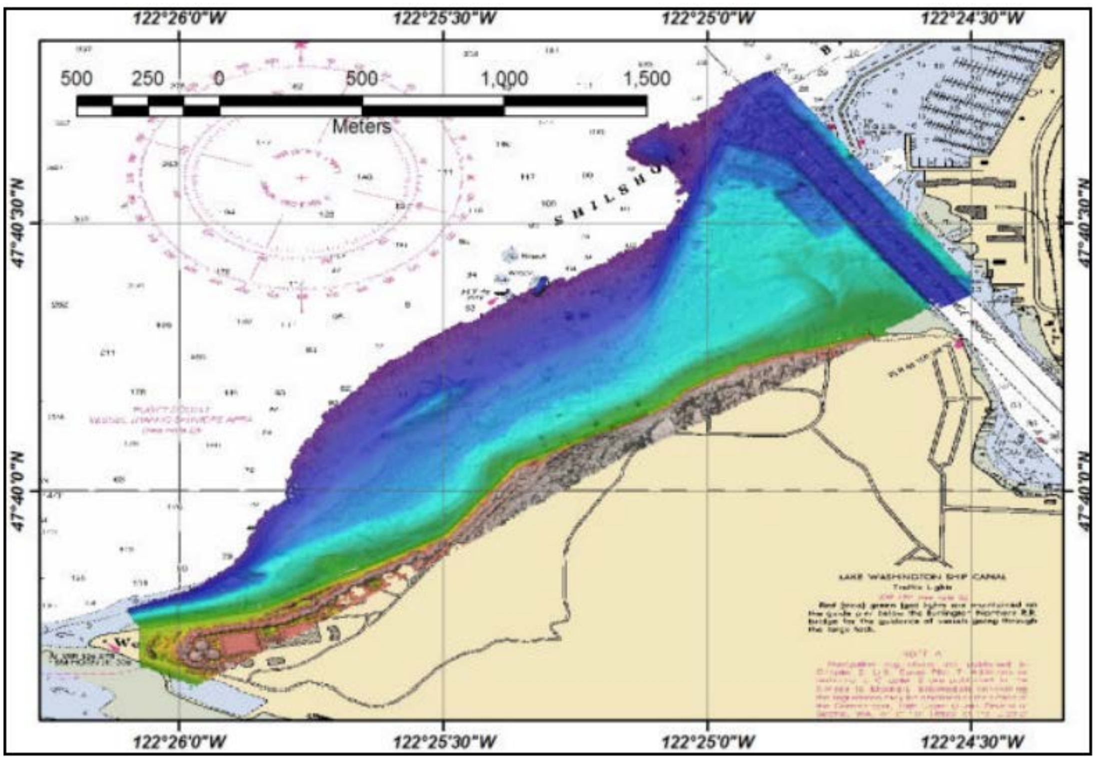

Figure 6.4.5. Shilshole Bay study site: Gridded bathymetry from the SHOALS-1000T survey overlaid on a NOAA Chart (Lockhart, Dushan, and Millar 2005).

In 2013, the Remote Sensing Division (RSD) in NOAA's National Geodetic Survey (NGS) procured a Riegl VQ-820-G to compliment the division's topo-bathy operations (namely, shoreline mapping). The goals for the performance evaluation were to evaluate depth penetration capability, vertical accuracy underwater and horizontal accuracy underwater. Similar to the USACE, NGS also adopted QL survey standards of the Interagency Working Group's National Coastal Mapping Strategy (Table 5.5; Figure 5.3.13). The ALB system was mounted on a DeHavilland Twin Otter (DHC-6) for both the geometric calibration and accuracy tests.

Geometric calibration flights were conducted after each installation of the sensor suite. An example of NOAA's geometric calibration conducted during June, 2013 over land (Sun City, FL) is described. The calibration site was selected in a suburban environment with many houses that have pitched roofs and open flat surfaces, such as cul-de-sac roads. The GPS baseline between the base station and aircraft are kept to a minimum, so that the uncertainties associated with the trajectory file are minimized (Figure 5.3.17). The raw data were initially processed to a point cloud referenced to an appropriate coordinate system. The average density of the laser measurements was around 40 measurements per square meter (#/m^2), and certain areas of the calibration site with high overlap had up to 180 $\#/m^2$ (Figure 5.3.18). The initial boresight angles were calculated and verified in a three-step procedure. First, an initial examination of the relative offset between adjacent scan lines is performed. The offset observed is utilized to assist in finding tie objects between different scans. A tie object is a planar surface, point, or sphere found in a scan. An observation consists of the matching of two similar objects in overlapping scans. Between 30,000 to 70,000 observations are typically identified for a geometric calibration flight. Second, the distances of the observations and a standard deviation are calculated for estimation of the current fit. Third, an adjustment is calculated for optimal boresight angles to achieve a best fit between all scans in the data set. The data is then reprocessed with the newly calculated boresight angles. The third step was repeated until the standard deviation of distances between objects converged to a value between 1 to 3 cm with further adjustment iterations providing negligible differences. Various techniques are utilized to analyze the results from qualitative examination of intensity data and hillshade images to look for unusual scan or geometrical artifacts to quantitative differences between flat surfaces in overlapping scans. The results from the Boresight Calibration procedure were verified using control points measured in cul-de-sac areas using rapid static GNSS field-surveys. The average difference from the comparison between the ALB survey to the control points was -0.012 cm vertical difference with a standard deviation of 0.039 m.

eCommons (2019) https://doi.org/10.7298/vfyq-3506

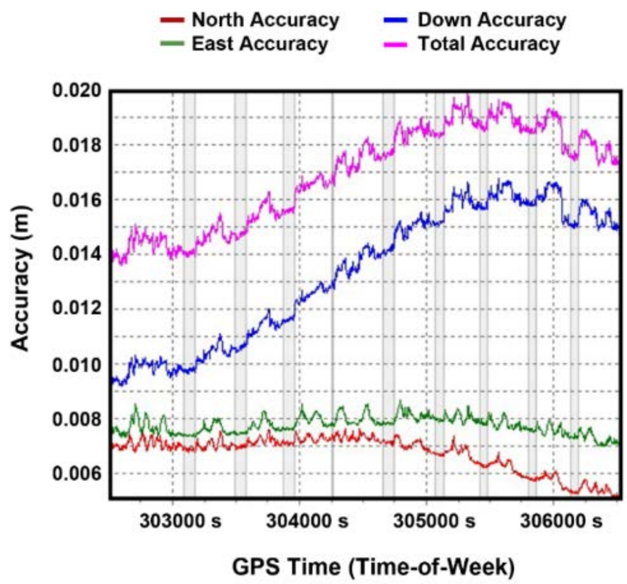

Figure 6.4.6. Initial accuracy of the aircraft during the Boresight Calibration procedure reported by Applanix POSPac. The vertical grey areas mark the periods during ALB acquisition and the spikes in accuracy indicate turning of the aircraft from one survey line to another.

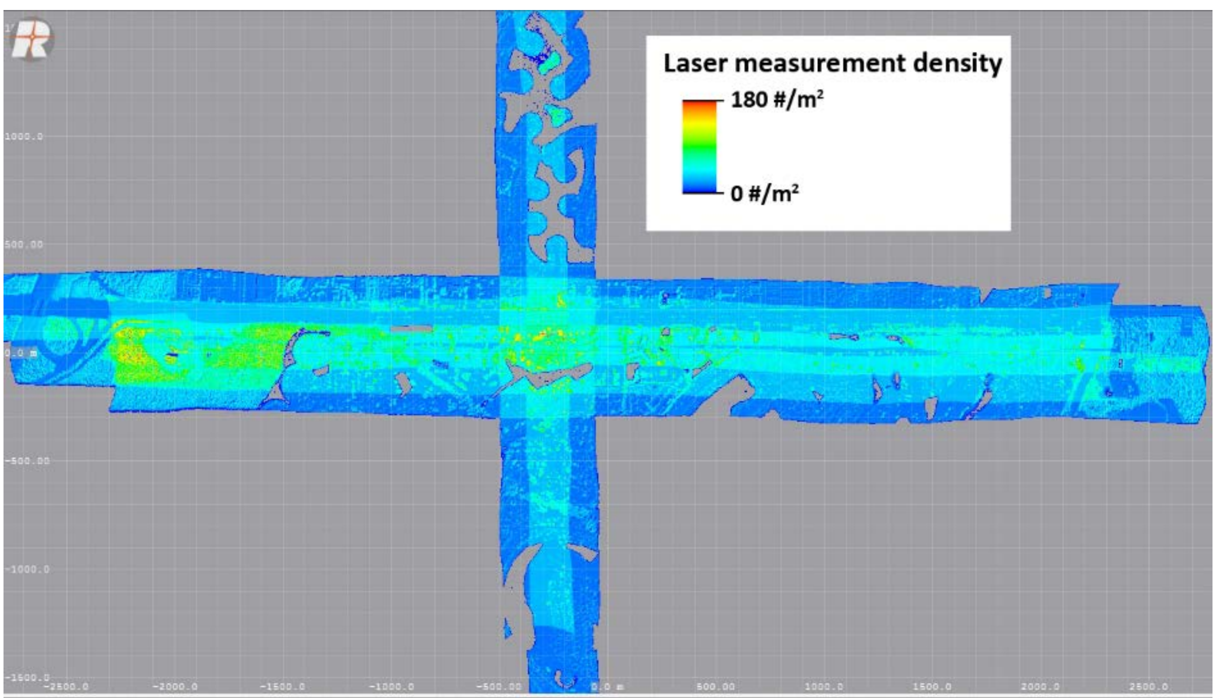

Figure 6.4.7. Density map of the Boresight Calibration site used for calculating the boresight angles for the Riegl VQ-820-G.

Next, a set of relative accuracy tests were conducted over coastal areas (from dry land into shallow bathymetry) and over offshore sites. The evaluation over coastal areas was conducted at Ft. DeSoto, FL

eCommons (2019) https://doi.org/10.7298/vfyq-3506

and Island Beach State Park, NJ. The ALB surveys were compared against Post Processing Kinematics (PPK) GPS and rapid static GNSS field-surveys. Shoreline transects were collected perpendicular to the shoreline using PPK GPS and rapid static GNSS field-surveys. The shallow-water survey transects were obtained by a field survey crew wading into approximately waist-deep waters with range-pole or wheel-mounted GNSS antenna. Based on 13,526 samples a mean offset of 4 cm was calculated with a standard deviation of 5.5 cm. The evaluation test over offshore sites compared the Riegl VQ-820-G ALB survey data that was collected in March, 2012 to a SHOALS 1000T survey collected by the USACE USACE/JALBTCX in January, 2012 over Ft. Lauderdale, FL. Figure 5.3.19 shows the difference values between SHOALS 1000T to VQ-820-G dataset Stable areas such as the upper beach face and roads agreed well between the two datasets and the difference between the two datasets was within the tolerance defined for accuracy test (typically, RMSE < 10 cm). However, the two ALB surveys were collected at different seasons resulting in a non-uniform difference, where the beach profile (i.e., the nearshore morphology) changed between the two surveys.

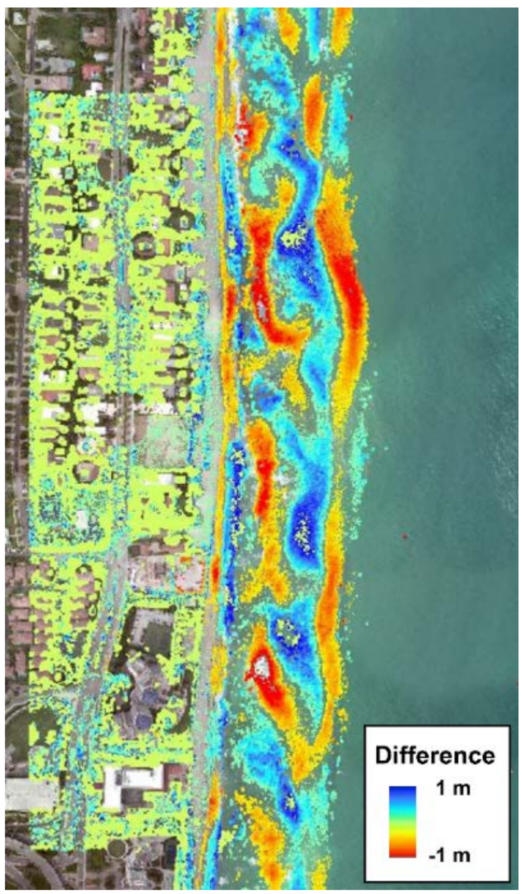

Figure 6.4.8. Difference map comparing a SHOALS-1000T survey to a Riegl VQ-820-G survey over Ft. Lauderdale, FL.

6.5 References

ASPRS. 2008a. “Common Lidar Data Exchange Format - LAS Industry Initiative 1.2.” http://www.asprs.org/a/society/committees/standards/asprs_las_format_v12.pdf.

———. 2008b. “LAS Specification, Version 1.4-R13.” Bethesda, MD: American Society of Photogrammetry and Remote Sensing. http://www.asprs.org/a/society/committees/standards/asprs_las_format_v12.pdf.

———. 2010. “LAS Specification: Version 1.3.-R11.” http://www.asprs.org/a/society/committees/standards/LAS_1_3_r11.pdf.

Beaudoin, Jonathan, Paul Johnson, and Ashton F Flinder. 2013. “R/V Falkor Multibeam Echosounder System Review.” Vol. Technical. Durham, NH: University of New Hampshire (UNH) Center for Coastal and Ocean Mapping (CCOM)/Joint Hydrographic Center (JHC). http://ccom.unh.edu/publications.

Chen, Yang, and Gérard Medioni. 1992. “Object Modelling by Registration of Multiple Range Images.” *Image and Vision Computing* 10 (3): 145–55. doi:10.1016/0262-8856(92)90066-C.

Dewberry. 2012. “National Enhanced Elevation Assessment.” http://www.dewberry.com/services/geospatial/national-enhanced-elevation-assessment.

El-Sheimy, Naser, Caterina Valeo, and Ayman Habib. 2005. *Digital Terrain Modeling: Acquisition, Manipulation, and Applications*. *Artech House Remote Sensing Library*. Norwood, MA: Artech House. http://library.books24x7.com/assetviewer.aspx?bookid=14812&chunkid=1&rowid=2.

Filin, Sagi. 2003. “Recovery of Systematic Biases in Laser Altimeters Using Natural Surfaces.” *Photogrammetric Engineering and Remote Sensing* 69 (11): 1235–42. http://eserv.asprs.org/PERS/2003journal/nov/2003_nov_1235-1242.pdf.

Fugro Pelagos. 2008. “Determination of SHOALS-100T Hydrographic Lidar TPU Model and Target Detection Test: Shilsole Bay, Puget Sound, WA.” Vol. Survey Rep. Sand Diego, CA: Fugro.

Gonsalves, Michael Oliver. 2010a. “A Comprehensive Uncertainty Analysis and Method of Geometric Calibration for a Circular Scanning Airborne Lidar.” Edited by Stephan Howden. *ProQuest Dissertations and Theses*. Hattiesburg, MS: The University of Southern Mississippi. http://search.proquest.com/docview/835075165/fulltextPDF/BB0E363A81F246C3PQ/1?accountid=10267.

———. 2010b. “Flat-Bottomed World You Make Thoselidar Swirls around: Contrasting a Ship-Based Acoustic Patch Test with an Automated Calibration Routine for a Circular-Scanning Airborne Lidar System.” In *Canadian Hydrographic Conference 2010*. Quebec, QC, Canada.

Habib, Ayman. 2009. “Accuracy, Quality Assurance, and Quality Control of LiDAR Data.” In *Topographic Laser Ranging and Scanning: Principles and Processing*, edited by Jie Shan and Charles K Toth, 269–94. Boca Raton, FL: CRC Press.

Habib, Ayman, A P Kersting, Ki In Bang, and Dong-Cheon Lee. 2010. “Alternative Methodologies for the Internal Quality Control of Parallel LiDAR Strips.” *Geoscience and Remote Sensing, IEEE Transactions On* 48 (1): 221–36. doi:10.1109/TGRS.2009.2026424.

IHO. 2008. “IHO Standards for Hydrographic Surveys.” Vol. S-44. Monaco: International Hydrographic Organization. http://www.thsoa.org/pdf/s44_4.pdf.

Imahori, Gretchen, Jeff Ferguson, Toshi Wozumi, David Dave Scharff, Shachak Pe’eri, Christopher E Parrish, Stephen A White, Inseong Jeong, Jon Sellars, M Aslaksen, et al. 2013. “A Procedure for Developing an Acceptance Test for Airborne Bathymetric Lidar Data Application to NOAA Charts in Shallow Waters.” *NOAA Technical Memorandum CS 32*. Vol. NOS CS-32. Silver Spring, MD: National Oceanographic and Atmospheric Administration. http://www.nauticalcharts.noaa.gov/csdl/publications/TM_NOS-CS32_FY13_Lidar.pdf.

Imahori, Gretchen, Jeff Ferguson, Toshi Wozumi, David Scharff, Shachak Pe’eri, Christopher E. Parrish, Stephen A. White, Inseong Jeong, Jon Sellars, and M. Aslaksen. 2013. “A Procedure for

Developing an Acceptance Test for Airborne Bathymetric Lidar Data Application to NOAA Charts in Shallow Waters." *NOAA Technical Memorandum CS 32*. Vol. NOS CS-32. Silver Spring, MD: National Oceanographic and Atmospheric Administration. http://www.nauticalcharts.noaa.gov/csdl/publications/TM_NOS-CS32_FY13_Lidar.pdf.

LaRocque, Paul E, John R Banic, and A G Cunningham. 2004. "Design Description and Field Testing of the SHOALS-1000 Airborne Bathymeter." In *Laser Radar Technology and Applications IX*, SPIE 5412:162–84. SPIE. doi:10.1117/12.564924.

Lockhart, Carol, Arumugam Dushan, and David Millar. 2005. "Meeting Hydrographic Charting Specifications with SHOALS-1000T Airborne Lidar Bathymeter." In *U.S. Hydro 2005*. San Diego, CA. http://www.thsoa.org/us05papers.htm.

Ocean Surveys, Inc. 2009. "Shallow Water Multibeam Hydrographic and Side Scan Sonar Survey." Vol. Field No: Old Saybrook, CT: NOAA/NOS/OCS Descriptive Report. http://surveys.ngdc.noaa.gov/mgg/NOS/coast/H10001-H12000/H11896/DR/H11896.pdf.

OCS. 2014. "FIeld Procedures Manual." National Oceanic and Atmospheric Administration: Office of Coast Survey. http://www.nauticalcharts.noaa.gov/hsd/fpm/2014_FPM_Final.pdf.

Optech. 2005. "Technical Report for JALBTCX." Vol. DACW42-01-. Toronto, Ontario, CA: Optech Incorporated.

Pe'eri, Shachak, Lynnette V Morgan, William D Philpot, and Andrew A Armstrong. 2011. "Land-Water Interface Resolved from Airborne LIDAR Bathymetry (ALB) Waveforms." *Journal of Coastal Research* SI 62. Coastal Education and Research Foundation: 75–85. doi:10.2112/SI_62_8.

Schenk, Toni. 2001. "Modeling and Recovering Systematic Errors in Airborne Laser Scanners." *Technical Notes in Photogrammetry*. Vol. 19. Columbus, Ohio: The Ohio State University.

Snyder, G. I. 2012. "National Enhanced Elevation Assessment at a Glance." Vol. U.S. Geolo. U.S.G.S. http://pubs.usgs.gov/fs/2012/3088/.

Toth, Charles K. 2009. "Strip Adjustment and Registration." In *Topographic Laser Ranging and Scanning: Principles and Processing*, edited by Jie Shan and Charles K Toth, 235–68. Boca Raton, FL: CRC Press, Taylor and Francis Group. http://www.crcnetbase.com/isbn/9781420051438.

USACE. 2012. "Scope of Work: National Coastal Mapping Program - Lake Michigan." Vol. EN Project. Kiln, MS: U.S. Corps of Engineers.

Vaughn, C R, J L Button, W B Krabill, and D Rabine. 1996. "Georeferencing of Airborne Laser Altimeter Measurements." *International Journal of Remote Sensing* 17 (11). Taylor & Francis: 2185–2200. doi:10.1080/01431169608948765.

Wehr, Aloysius. 2009. "LiDAR Systems and Calibration." In *Topographic Laser Ranging and Scanning: Principles and Processing*, edited by Jie Shan and Charles K Toth, 129–72. Boca Raton, Florida: CRC Press, Taylor and Francis Group. ftp://ftp.ecn.purdue.edu/jshan/Zproject/proofs/04/51423_C004_corr.pdf.

White, Stephen. 2007. "Utilization of Lidar and NOAA's Vertical Datum Transformation Tool (VDatum) for Shoreline Delineation." In *Marine Technology Society/IEEE Oceans Conference*. Vancouver, BC: IEEE. doi:10.1109/OCEANS.2007.4449147.

Wozencraft, Jennifer M. 2010. "Requirements for the Coastal Zone Mapping and Imaging Lidar (CZMIL)." In *Algorithms and Technologies for Multispectral, Hyperspectral, and Ultraspectral Imagery XVI, April 5, 2010 - April 8*, SPIE 7695:The Society of Photo-Optical Instrumentation Engin. Orlando, FL: SPIE. doi:10.1117/12.851891.

———. 2014. "USACE Information Products."